THE JOURNAL OF BIOLOGICAL CHEMISTRY VOL. 280, NO. 40, pp. 34105–34112, October 7, 2005

Selective Vulnerability of Dopaminergic Neurons to Microtubule Depolymerization*

Received for publication, March 30, 2005, and in revised form, July 18, 2005 Published, JBC Papers in Press, August 9, 2005, DOI 10.1074/jbc.M503483200

Yong Ren, Wenhua Liu, Houbo Jiang, Qian Jiang, and Jian Feng[1]

From the Department of Physiology and Biophysics, State University of New York, Buffalo, New York 14214

Parkinson disease (PD) is characterized by the specific degeneration of dopaminergic (DA) neurons in substantia nigra and has been linked to a variety of environmental and genetic factors. Rotenone, an environmental PD toxin, exhibited much greater toxicity to DA neurons in midbrain neuronal cultures than to non-DA neurons. The effect was significantly decreased by the microtubule-stabilizing drug taxol and mimicked by microtubule-depolymerizing agents such as colchicine or nocodazole. Microtubule depolymerization disrupted vesicular transport along microtubules and caused the accumulation of dopamine vesicles in the soma. This led to increased oxidative stress due to oxidation of cytosolic dopamine leaked from vesicles. Inhibition of dopamine metabolism significantly reduced rotenone toxicity. Thus, our results suggest that microtubule depolymerization induced by PD toxins such as rotenone plays a key role in the selective death of dopaminergic neurons.

At the cellular level Parkinson disease is characterized by the selective degeneration of dopaminergic neurons in substantia nigra. A variety of genetic and environmental factors contribute to such a specific loss. Long term epidemiological studies have indicated that exposure to agricultural pesticides represents a significant risk factor for Parkinson disease (1). It has been found recently that long term, systemic administration of rotenone, a natural substance widely used as a pesticide, produces selective degeneration of dopaminergic neurons and PD[2]-like locomotor symptoms in rats (2).

Rotenone is a membrane-permeable compound that has two known molecular targets in the cell; it inhibits complex I in the mitochondrial respiratory chain (3) and depolymerizes microtubules (4, 5). The former activity has been studied extensively but could not fully explain the specificity of rotenone toxicity on DA neurons, as rotenone infusion uniformly inhibits complex I in all brain areas (2). Although the latter activity causes microtubule depolymerization in every type of cells, the consequence would be quite different. Nigral dopaminergic neurons send very long axons to striatum to control voluntary locomotor activity. Axonal transport of vesicles are mediated by microtubule-based motor proteins (6). Microtubule depolymerization would disrupt vesicular transport and cause the accumulation of vesicles in the soma. In the case of DA neurons, the cargo is dopamine, whose oxidation produces large quantities of reactive oxygen species and may trigger cell death (7). Other types of cells that do not have extensive processes or do not contain an oxidizable neurotransmitter (*e.g.* glutamatergic or GABAergic neurons) would be spared even though their microtubules are depolymerized by rotenone to a similar extent. In the present study we attempt to elucidate the role of microtubule depolymerization in the selective toxicity of rotenone on DA neurons.

EXPERIMENTAL PROCEDURES

Antibodies and Reagents—Rabbit anti-TH was from Affinity BioReagents (Golden, CO). Mouse anti-TH was from Pel-Freez (Rogers, AK). Mouse anti-NeuN or anti-GAD, guinea pig anti-vGlut2, and rabbit anti-GAT1 were from Chemicon (Temecula, CA). Mouse antibodies against FLAG, syntaxin I, or synaptophysin as well as fluorescein isothiocyanate- or rhodamine-conjugated secondary antibodies against mouse, rabbit, or sheep were from Sigma. Cy5-conjugated anti-mouse antibody was from Amersham Biosciences. Alexa Fluor 488-conjugated anti-guinea pig IgG was from Molecular Probes (Eugene, OR). Apoptosis was detected by **T**dT-mediated d**U**TP-X **n**ick **e**nd **l**abeling (TUNEL) staining using a kit from Roche Applied Science.

Midbrain Neuronal Culture, Image Acquisition, and Quantification—Primary midbrain neuronal cultures were prepared from rat embryos at E18 as previously described (8). Cultures on coverslips were maintained in 12-well plates in neurobasal media supplemented with 2% B27 (Invitrogen) and AraC (5 μM, Sigma) for 14 days before they were treated with various drugs. Treated neuronal cultures were fixed and stained as previously described (9). In experiments with TUNEL staining, the reaction was performed for 1 h at 37 °C before incubation with antibodies. Green, red, or blue signals in all images represented fluorescence from fluorescein isothiocyanate, rhodamine, or Cy5 channels, respectively. In some experiments, treated midbrain cultures were stained in culture media containing 4 μg/ml propidium iodide (PI; from Sigma) for 5 min at 37 °C in the dark. After the cultures were washed three times in PBS, they were fixed, permeabilized, and stained with relevant antibodies as described previously (9). Fluorescence images on cell death were acquired on a Nikon fluorescence microscope with a CCD camera (Diagnostic Instrument, Sterling Heights, MI), and merged using the software SPOT (Diagnostic Instrument). For each condition, at least three coverslips from independent experiments were examined. All TH^+ neurons on a coverslip (100–200) were counted together with a random selection of 120–250 TH^- neurons. Images on microtubule morphology and vesicle accumulation were acquired on a confocal microscope from Bio-Rad.

Quantification of synaptophysin or syntaxin I intensity was performed using NIH Image J. The contour of the soma was drawn manually. The degree of synaptophysin or syntaxin I accumulation in the cell body was calculated by dividing the intensity of background-subtracted signal within the border by its area. At least 10 TH^+ and 10 TH^- neurons were analyzed for each coverslip, and at least 3 coverslips were used for each treatment. There was no significant difference between TH^+

* This work is supported by National Institutes of Health Grant NS41722 (to J. F.). The costs of publication of this article were defrayed in part by the payment of page charges. This article must therefore be hereby marked "*advertisement*" in accordance with 18 U.S.C. Section 1734 solely to indicate this fact.

[1] To whom correspondence should be addressed: Dept. of Physiology and Biophysics, State University of New York at Buffalo, 124 Sherman Hall, Buffalo, NY 14214. Tel.: 716-829-2345; Fax: 716-829-2699; E-mail: jianfeng@buffalo.edu.

[2] The abbreviations used are: PD, Parkinson disease; DA, dopamine; vGlut2, vesicular glutamate transporter 2; TH, tyrosine hydroxylase; VMAT2, vesicular monoamine transporter 2; TUNEL, TdT-mediated dUTP-X nick end labeling; MAO, monoamine oxidase; MES, 2-(*N*-morpholino)ethanesulfonic acid; GABA, γ-aminobutyric acid; PIPES, 1,4-piperazinediethanesulfonic acid; ROS, reactive oxygen species.

and TH^- neurons with regard to accumulation of these puncta in response to rotenone or colchicine. All data were expressed as the mean ± S.E. Statistical analyses were performed with unpaired *t* test using the software Origin (Origin Lab, Northampton, MA).

Measurement of Protein Carbonyls—Midbrain neuronal cultures were treated with various agents for 4 h under culture conditions, washed 3 times in PBS, and lysed in cold lysis buffer (0.5% v/v Nonidet P-40, 1 M Tris, pH 8.0, 150 mM NaCl, 50 mM NaF, 10% v/v glycerol, 0.5 M EDTA, and 0.1 M Na_3VO_4). In some experiments midbrain slices (400 μm thick) from 3–4-week-old male SD rats were cut on a vibratome as described before (10). Slices were treated with various agents for 2 h at room temperature under constant oxygenation (95% O_2, 5% CO_2) in a buffer containing 126 mM NaCl, 2.5 mM KCl, 2 mM $CaCl_2$, 2 mM $MgCl_2$, 26 mM $NaHCO_3$, 1.25 mM NaH_2PO_4, 1 mM pyruvic acid, and 10 mM glucose, pH 7.4 (300–305 mosmol/liter). Treated slices were homogenized in cold lysis buffer described above. Protein carbonyls were measured with the Oxyblot protein oxidation detection kit (Chemicon) as described before (11). Briefly, 10 μg of proteins from total cell lysates were incubated with an equal volume of 12% SDS and 2 volumes of 2,4-dinitrophenylhydrazine solution for 15 min at room temperature and then with 1.5 volumes of neutralization solution to stop the reaction. The samples were spotted on a nitrocellulose membrane, dried, and cross-linked with a UV Crosslinker (Stratagene, La Jolla, CA). Membranes were Western-blotted with an antibody against 2,4-dinitrophenyl to detect protein carbonyls that are derivatized by 2,4-dinitrophenylhydrazine. Intensities of the dots were quantified with NIH Image J by measuring signals in a preset circle of the same size.

Measurement of Free or Polymerized Tubulin in the Cell—Free or polymerized tubulin from midbrain neuronal cultures was extracted using a standard protocol (12). Briefly, midbrain neuronal cultures maintained in 3.5-cm dishes in vitro for 14 days were washed twice at 37 °C with 1 ml of Buffer A containing 0.1 M MES, pH 6.75, 1 mM $MgSO_4$, 2 mM EGTA, 0.1 mM EDTA, and 4 M glycerol. After the cultures were incubated at 37 °C for 5 min in 600 μl of free tubulin extraction buffer (Buffer A plus 0.1% v/v Triton X-100 and protease inhibitors), the extracts were centrifuged at 37 °C for 2 min at 16,000 × *g*. The supernatant fractions contained free tubulin extracted from the cytosol. The pellet fraction and lysed cells in the culture dish were dissolved in 600 μl of 25 mM Tris, pH 6.8, plus 0.5% SDS and contained tubulin originally in a polymerized state (*i.e.* as microtubules). Equal amounts of total proteins from free or polymerized tubulin fractions were analyzed by Western blotting with anti-α-tubulin antibody (Sigma). The intensity of tubulin bands was quantified from three different experiments with the software NIH imaging.

Tubulin Polymerization Assay—The assay was performed using a standard protocol described before (13). Briefly, purified tubulin (>99% purity, from Cytoskeleton, Denver, CO) was mixed on ice with varying concentrations of rotenone in PEM buffer (0.1 M PIPES, 1 mM $MgSO_4$, and 1 mM EGTA) with 20% glycerol and 1 mM GTP. The final concentration of tubulin was kept at 5.0 mg/ml. After 15 min of incubation on ice, the mixture was placed at 37 °C, and light absorbance at 340 nm was monitored continuously on a Shimadzu UV160U spectrometer with temperature control. Turbidity of the solution reflects the degree of tubulin polymerization. The experiment was repeated three times with similar results.

Tubulin-[^{3}H]Dihydrorotenone Binding Assay—Binding of [^{3}H]dihydrorotenone to tubulin was determined by the DEAE-cellulose filter assay according to the procedure of the [^{3}H]colchicine-tubulin binding assay described previously (14, 15). The assay was conducted in 50 μl of binding buffer (0.1 M PIPES, 1 mM EGTA, 1 mM $MgSO_4$, 0.1 mM GTP, pH 6.8) containing 20 μg purified tubulin (Cytoskeleton) and an appropriate amount of [^{3}H]dihydrorotenone (60 Ci/mmol, American Radiolabeled Chemicals, St. Louis, MO). After incubation at room temperature for 1 h, the mixture was applied onto a pre-wetted stack of 4 DE81 DEAE-cellulose filter discs (2.3 cm in diameter). The filter stack was washed 10 min later with 40 ml of cold binding buffer containing 0.1 M KCl and then placed in 10 ml of scintillation fluid to measure the radioactivity bound to tubulin on DE81 discs. Nonspecific binding was determined with the same amount of bovine serum albumin in place of tubulin. In some experiments, a 200-fold excess of unlabeled rotenone or colchicine was preincubated with tubulin for 30 min at room temperature before the addition of [^{3}H]dihydrorotenone. All experiments were repeated three times with similar results.

RESULTS

Rotenone Has a Much Higher Toxicity on TH^+ Neurons Than on TH^- Neurons—Long term systemic administration of rotenone causes selective degeneration of nigral DA neurons in rats (2). To study the mechanism underlying the specific toxicity of rotenone, we treated rat embryonic midbrain neurons cultured for 14 days with various concentrations of rotenone for 12 h. Most of the neurons expressing tyrosine hydroxylase (TH) in such cultures are dopaminergic neurons. We co-stained fixed cultures with antibodies against TH and the neuronal nuclear marker NeuN to highlight TH^+ and TH^- neurons. TUNEL staining was used to label cells undergoing apoptosis. Rotenone induced apoptosis and broken processes in TH^+ neurons, whereas most of the TH^- neurons in the same culture were unaffected (Fig. 1*B*). As shown in Fig. 1*C*, rotenone caused significant apoptosis of TH^+ neurons at all concentrations tested ($p < 0.01$, *versus* control, $n = 3\sim10$ coverslips for each condition) but produced much less apoptosis in TH^- neurons. The differential effects of rotenone were also observed when neuronal death was quantified by staining with PI, a membrane-impermeable fluorescent dye that labels nuclear DNA in dead cells (Fig. 1*D*). With this readout, higher percentages of TH^- neurons were killed by rotenone compared with results from TUNEL staining. This suggests that, at rotenone concentrations above 1 μM both apoptosis and necrosis are induced in the cell.

To substantiate these results, we examined the time-course of rotenone-induced cell death in TH^+ and TH^- neurons. When midbrain neuronal cultures were treated with 10 nM rotenone, almost all TH^+ neurons were killed by 24 h. In contrast, the percentages of apoptotic TH^- neuron were much lower at all time points examined (Fig. 1*E*). Similar results were obtained when cell death was quantified by PI-staining (data not shown). We also examined the time-course of cell death in response to 10 μM rotenone. Both PI staining (Fig. 1*F*) and TUNEL staining (data not shown) produced similar results, that TH^+ neurons were much more sensitive than TH^- neurons to rotenone toxicity at 12 through 72 h.

To confirm the specificity of rotenone toxicity, we examined the death of major neuronal populations in the same cultures by using antibodies against GABA transporter-1 (GAT-1) or vesicular glutamate transporter 2 (vGlut2) to label GABAergic or glutamatergic neurons, respectively. Rotenone produced very mild toxicity on GABAergic or glutamatergic neurons, which was similar to that on TH^- neurons but was much lower than that on TH^+ neurons (Fig. 1*G*). Furthermore, we examined rotenone toxicity on cortical neuronal cultures, which contained mostly glutamatergic or GABAergic neurons but very few TH^+ neurons. As shown in Fig. 1*H*, the toxicity of rotenone on TH^- neurons in cortical cultures was very mild and almost the same as TH^- neurons in midbrain cultures, which was much lower than that on TH^+ neurons. Together,

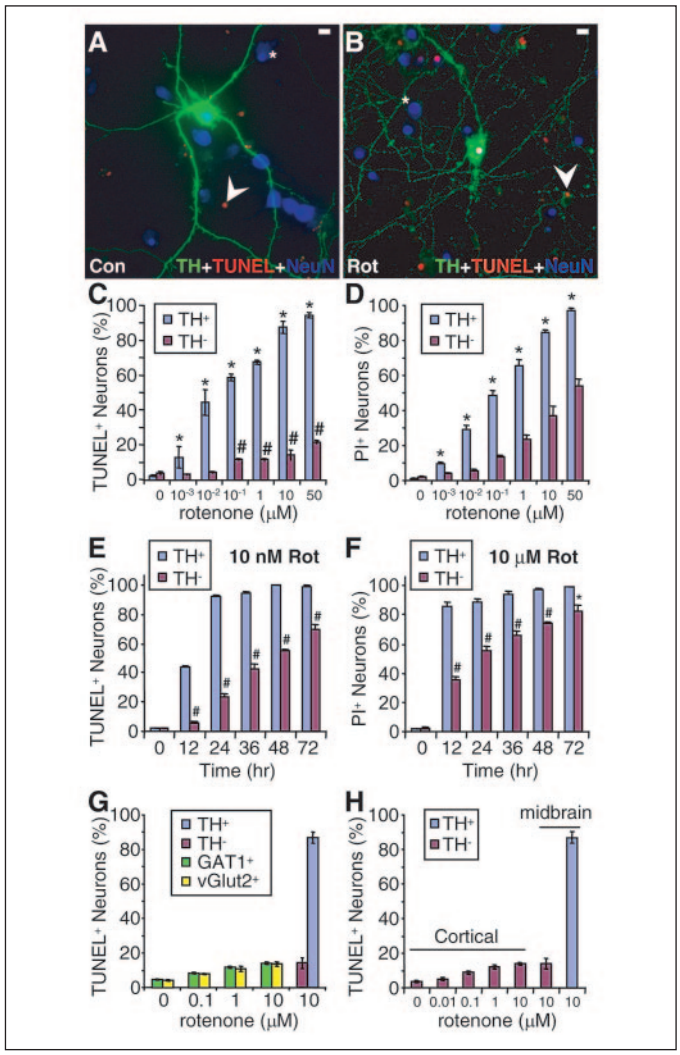

FIGURE 1. **Rat midbrain TH$^+$ neurons exhibited much greater vulnerability than TH$^-$ neurons to rotenone.** *A–C*, embryonic midbrain neuronal cultures treated with various concentrations of rotenone (*Rot*) for 12 h were co-stained for TH (*green*), TUNEL (*red*), and NeuN (*blue*). Representative images at 0 (*A*) or 10 μM (*B*) rotenone were shown. *, TH$^-$ neurons; *arrowheads*, dead glial cells; *bars*, 10 μm. Rotenone induced apoptosis of TH$^+$ neurons in a dose-dependent manner but caused minimal death of TH$^-$ neurons only at high concentrations (*C*). *Con*, control. * and #, $p < 0.01$, $n = 3\sim10$, *versus* control for TH$^+$ or TH$^-$ neurons, respectively. *D*, rotenone-induced neuronal death was quantified by staining with PI. The percentages of PI$^+$ neurons were significantly higher in TH$^+$ neurons than in TH$^-$ neurons at all rotenone concentrations tested. *, $p < 0.01$, $n = 3\sim6$, TH$^+$ *versus* TH$^-$ neurons. *E* and *F*, time-course of cell death induced by 10 nM (*E*) or 10 μM (*F*) rotenone, as quantified by TUNEL (*E*) or PI (*F*) staining. Rotenone toxicity was significantly higher in TH$^+$ than in TH$^-$ neurons at each time point. #, $p < 0.001$; *, $p < 0.05$; $n = 3$ *versus* TH$^+$ neurons. *G*, in midbrain neuronal cultures rotenone toxicity on GABAergic (GAT1$^+$), glutamatergic (vGlut2$^+$) or TH$^-$ neurons was very similar but much lower than that on TH$^+$ neurons ($p < 0.001$, $n = 3$). *H*, the mild toxicity of rotenone was very similar on TH$^-$ neurons from cortical or midbrain cultures but was much lower than that on TH$^+$ neurons from midbrain cultures ($p < 0.001$, $n = 3$). For all experiments involving quantification of neuronal death, *n* equals the number of coverslips for each condition. All TH$^+$ neurons (100–200) on a coverslip were counted together with a random selection of 120–250 TH$^-$ neurons or about 200 GAT1$^+$ or vGlut2$^+$ neurons.

our results above demonstrated the much higher toxicity of rotenone on TH$^+$ neurons compared with TH$^-$ neurons including GABAergic or glutamatergic neurons.

The Selective Toxicity of Rotenone on TH$^+$ Neurons Is Dependent on Its Microtubule-depolymerizing Activity—Rotenone treatment (10 μM for 12 h) depolymerized microtubules in all neurons, producing shrunk and broken processes (Fig. 2*B*). Co-application of taxol (10 μM), a well established microtubule-stabilizing drug, significantly blocked rotenone-induced apoptosis and restored normal morphology of the processes and microtubules inside (Fig. 2*C*). As summarized in Fig. 2*D*, the selective toxicity of rotenone at 10 nM or 10 μM was significantly reduced by 100 nM or 10 μM taxol, respectively ($p < 0.01$, $n = 4\sim8$ coverslips for each condition). No significant toxicity was found for taxol compared with the control ($p > 0.05$, $n = 4$). On the other hand, the effect of taxol and rotenone co-treatment (both at 10 μM) on TH$^-$ neurons (9.0 ± 1.4%) was not significantly different from the mild toxicity of 10 μM rotenone alone (14.2 ± 3.1%, $p > 0.20$, $n = 6\sim8$). Low concentrations of rotenone (10 nM) had no significant toxicity on TH$^-$ neurons (Fig. 1*C*).

To confirm that microtubule depolymerization did cause specific death of TH$^+$ neurons, we treated midbrain cultures with colchicine, a well characterized microtubule-depolymerizing agent. Colchicine (10 μM for 12 h) induced significant apoptosis in TH$^+$ but not TH$^-$ neurons (Fig. 2*F*). Co-application of taxol (10 μM) greatly reduced colchicine toxicity (Fig. 2*G*). Colchicine-induced microtubule depolymerization led to shrunk and broken processes (Fig. 2*F*), very similar to the situation with rotenone treatment (Fig. 2*B*). Co-treatment with taxol prevented microtubule depolymerization and restored normal morphology of the processes and microtubules (Fig. 2*G*). As summarized in Fig. 2*H*, colchicine-induced apoptosis of TH$^+$ neurons was almost completely blocked by taxol ($p < 0.001$, $n = 4\sim9$). On the other hand, the effect of colchicine (10 μM) on TH$^-$ neurons (6.70 ± 1.12%) was not significantly different from the control (4.26 ± 1.11%, $p > 0.15$, $n = 4\sim9$) and was not significantly changed by taxol co-treatment (5.08 ± 1.67%, $p > 0.40$, $n = 4\sim9$). We found that colchicine selectively killed TH$^+$, but not TH$^-$, neurons in a dose-dependent manner from 1 nM to 50 μM (data not shown).

To further substantiate our findings, we treated midbrain neuronal cultures with a different microtubule-depolymerizing agent, nocodazole, at 10 μM for 12 h. As summarized in Fig. 2*H*, nocodazole induced apoptosis of TH$^+$ neurons (39.0 ± 3.7%, $n = 3$) to a similar extent as that by colchicine (44.5 ± 4.1%, $n = 9$, $p > 0.05$). The toxicity of nocodazole was greatly reduced by co-application of 10 μM taxol (10.2 ± 0.8%, $n = 3$, $p < 0.01$). In contrast, the toxicity of nocodazole on TH$^-$ neurons (4.78 ± 0.88%, $n = 3$) was much less than that on TH$^+$ neurons and was not significantly different from the Me_2SO vehicle control (4.26 ± 1.11%, $n = 9$, $p > 0.10$). Together, these lines of evidence suggest that microtubule depolymerization has much higher toxicity in TH$^+$ neurons than in TH$^-$ neurons.

Rotenone Toxicity Is Contributed Both by Its Microtubule-depolymerizing Activity and by Its Ability to Inhibit Complex I—The toxicity of colchicine or nocodazole on TH$^+$ neurons was more specific, but weaker, than that of rotenone. If this difference is due to the complex I-inhibiting activity of rotenone, then the combination of a pure complex I inhibitor and a pure microtubule-depolymerizer might mimic the effect of rotenone. To test this hypothesis, we chose amytal, a complex I inhibitor with no known effect on microtubules. Amytal treatment (10 μM for 12 h) induced a moderate level of apoptosis in TH$^+$ neurons without significantly affecting microtubules (Fig. 3*B*). Co-application of amytal and colchicine (10 μM for 12 h) markedly increased apoptosis in TH$^+$, but not in TH$^-$, neurons (Fig. 3*C*). Microtubule depolymerization was evident, and neuronal processes were fragmented (Fig. 3*C*). The toxicity of amytal was not significantly reduced by co-treatment with taxol (10 μM) (Fig. 3*D*).

As summarized in Fig. 3*E*, the combination of amytal and colchicine (64.5 ± 4.0%, $n = 4$) was significantly more toxic than either agent alone (44.5 ± 4.1%, $n = 9$, for colchicine; 32.2 ± 5.6%, $n = 8$, for amytal; $p <$ 0.01, double *versus* single treatments) and was equivalent to rotenone at 1 μM (67.0 ± 11.6%, $n = 3$, $p > 0.05$) but much less than the toxicity of

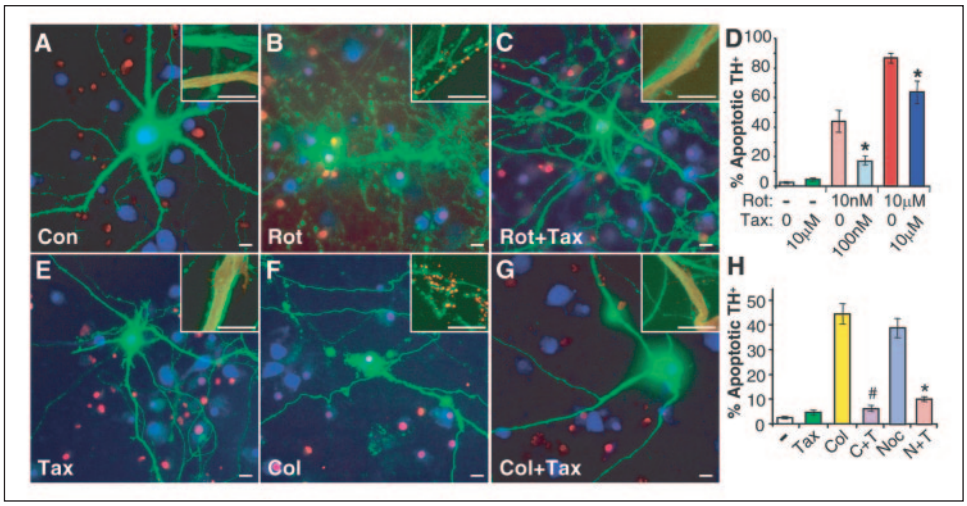

FIGURE 2. **The selective toxicity of rotenone on TH$^+$ neurons was significantly reduced by the microtubule-stabilizing drug taxol and mimicked by microtubule-depolymerizing drugs colchicine and nocodazole.** *A–C*, midbrain neuronal cultures were treated for 12 h without (*A*) or with (*B*) 10 μM rotenone (*Rot*) or rotenone plus taxol (*Tax*; *C*) and co-stained for TH (*green*), TUNEL (*red*), and NeuN (*blue*). *Insets* were enlarged portions of proximal processes co-stained with antibodies against α-tubulin (*green*) and TH (*red*) to show morphology of microtubules and processes. *Bars*, 10 μm. *D*, the selective toxicity of rotenone on TH$^+$ neurons at low (10 nM) or high (10 μM) concentration was significantly attenuated by co-application of taxol (100 nM or 10 μM, respectively). *, $p < 0.01$, $n = 4\sim8$, *versus* rotenone alone for the corresponding concentration. *E–G*, midbrain neuronal cultures were treated for 12 h with taxol (*E*), colchicine (*F*), or colchicine plus taxol (*G*) (all at 10 μM) and co-stained as above. *H*, the toxic effect of colchicine on TH$^+$ neurons mimicked that of rotenone and was almost totally blocked by taxol (*C+T*). Another microtubule-depolymerizing agent, nocodazole (*Noc*, 10 μM), had a similar effect, which was also greatly attenuated by taxol (*N+T*, both at 10 μM). #, $p < 0.001$, $n = 4\sim9$, *versus* colchicine; *, $p < 0.01$, $n = 3$, *versus* nocodazole.

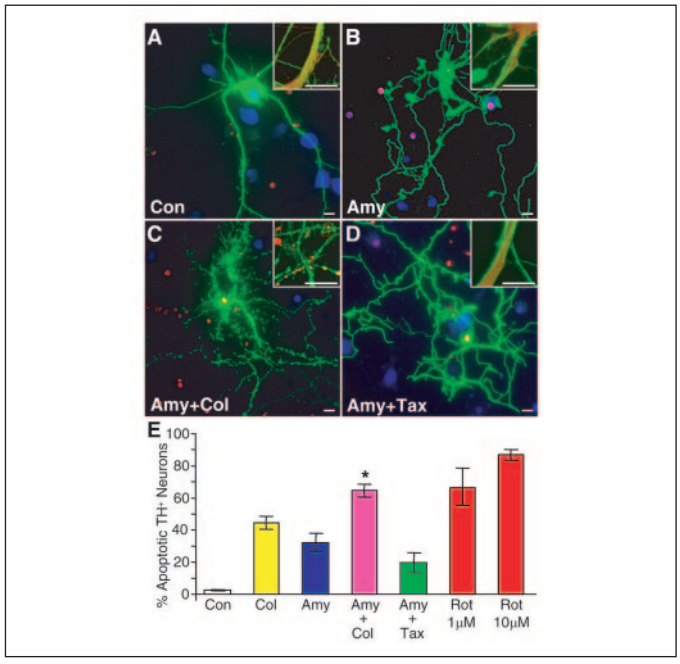

FIGURE 3. **Rotenone toxicity was dependent on its abilities to inhibit complex I and to depolymerize microtubules.** *A–D*, midbrain cultures were treated for 12 h without (*A*) or with (*B*) 10 μM amytal, amytal plus colchicine (*Col*; *C*), or amytal (*Amy*) plus taxol (*Tax*; *D*) and co-stained for TH (*green*), TUNEL (*red*) and NeuN (*blue*). *Con*, control. *Insets* were enlarged portions of processes co-stained with antibodies against α-tubulin (*green*) and TH (*red*) to show microtubules and processes. *Bars*, 10 μm. *E*, toxicity of amytal plus colchicine on TH$^+$ neurons was greater than that seen with either agent alone (*, $p < 0.01$, *Amy+Col versus Amy* or *Col* alone, $n = 4\sim9$). Toxicity of amytal was not significantly changed by taxol ($p > 0.15$, *Amy+Tax versus Amy*, $n = 8$).

10 μM rotenone (86.8 ± 3.4%, $n = 8$). The additive effect in the dual treatment suggests that colchicine and amytal act on different sites that independently contribute to cell death. This was corroborated by the result that taxol did not significantly alleviate amytal toxicity on TH$^+$ neurons ($p > 0.15$, amytal plus taxol (19.7 ± 6.2%, $n = 8$) *versus* amytal alone (32.2 ± 5.6%, $n = 8$)).

Rotenone Depolymerizes Microtubules in Neuronal Cultures, Blocks in Vitro Polymerization of Tubulin, and Binds to Purified Tubulin Directly—To directly compare the impact of rotenone, colchicine, and amytal (all at 10 μM) on microtubules, we measured the amount of free or polymerized tubulin in midbrain neuronal cultures treated without or with these agents for 30 min at 37 °C. Cells were gently lysed at 37 °C in a low concentration of detergent (0.1% v/v Triton X-100) to extract free tubulin while not disturbing polymerized tubulin in microtubules. As shown in Fig. 4*A*, the amount of free tubulin was greatly increased in response to rotenone (4.90 ± 0.42-fold of the control, $n = 3$ experiments, $p < 0.001$) or colchicine (5.00 ± 0.42-fold, $n = 3$, $p < 0.001$). In contrast, amytal did not significantly change the amount of free tubulin (1.02 ± 0.13-fold, $n = 3$, $p > 0.80$), confirming its lack of effect on microtubules. Incubation with taxol (10 μM for 10 min) before the addition of rotenone or colchicine completely blocked the effects of rotenone or colchicine. Reciprocal changes were observed in the amounts of polymerized tubulin (Fig. 4*A*).

We also examined the effect of low concentrations of rotenone on microtubules using this assay, since rotenone concentrations in the brain of the rat PD model are estimated to be 20–30 nM (2). As shown in Fig. 4*B*, rotenone significantly increased the amount of free tubulin at 10 nM (1.61 ± 0.19-fold of the control, $n = 3$, $p < 0.01$) and 100 nM (3.97 ± 0.39-fold, $n = 3$, $p < 0.01$). The microtubule-depolymerizing effects of rotenone at these low doses appear to be similar to or stronger than those of colchicine at the corresponding concentrations (10 nM colchicine, 1.23 ± 0.06-fold; 100 nM colchicine, 2.08 ± 0.23-fold; $n = 3$). At 10 μM, both rotenone and colchicine had similar potency in inducing microtubule depolymerization. Reciprocal changes were observed in the amounts of polymerized tubulin in microtubules (Fig. 4*B*).

Next, we performed *in vitro* biochemical experiments to show that the effect of rotenone on microtubules is direct rather than through its complex I-inhibiting activity, which produces reactive oxygen species in cells. Using purified bovine tubulin (>99% purity) from a commercial source (Cytoskeleton, Inc.), we examined the effect of rotenone on the *in vitro* polymerization of tubulin into microtubules, which was monitored by the turbidity of the solution ($A_{340\ nm}$). As shown in Fig. 4*C*,

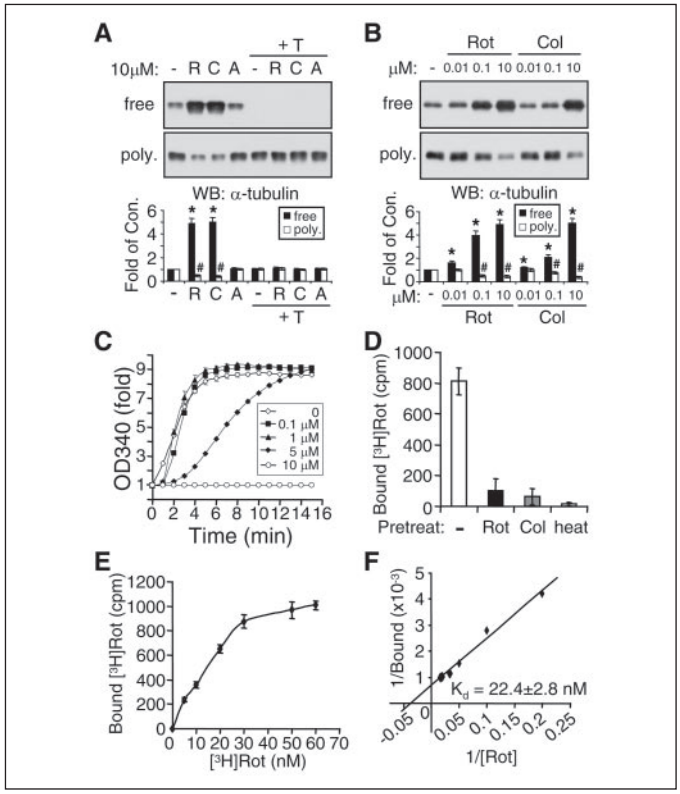

FIGURE 4. **Rotenone depolymerized microtubules in midbrain neuronal cultures, attenuated tubulin polymerization *in vitro*, and directly bound to purified tubulin.** *A*, midbrain neuronal cultures were treated with rotenone (*R*), colchicine (*C*), amytal (*A*), or taxol (10 μM for 30 min) as indicated. Rotenone or colchicine greatly increased free tubulin (*T*) and decreased polymerized (*poly.*) tubulin. Amytal had no significant effect, whereas taxol completely blocked the effect of rotenone or colchicine. * and #, $p < 0.001$, $n = 3$ experiments, *versus* the control for free or polymerized tubulin, respectively. *WB*, Western blot. *Con*, control. *B*, the microtubule-depolymerizing activity of rotenone (*Rot*) or colchicine (*Col*) was compared at 10 nM, 100 nM, and 10 μM. The effects of rotenone were similar to or stronger than those of colchicine at the corresponding doses. *, $p < 0.01$, $n = 3$, *versus* control for free tubulin; #, $p < 0.05$, *versus* control for polymerized tubulin. *C*, *in vitro* polymerization of purified tubulin was monitored by measuring turbidity ($A_{340\ nm}$) against incubation time at 37 °C. Rotenone directly attenuated tubulin polymerization in a dose-dependent manner. *D*, *in vitro* binding assay between purified tubulin and [^{3}H]dihydrorotenone without or with a pretreatment of unlabeled rotenone or colchicine (200-fold excess) or with heat-inactivated tubulin. *E*, [^{3}H]dihydrorotenone bound to tubulin in a dose-dependent and saturable manner. *F*, Scatchard analysis of the data in *E* from three separate experiments.

rotenone inhibited the self-assembly of tubulin in a dose-dependent manner. The result is very similar to a previous study (5).

To demonstrate that rotenone binds directly to tubulin, we utilized the standard DEAE-cellulose filter binding assay originally developed to measure the binding of tubulin and [^{3}H]colchicine (14, 15). Purified bovine tubulin (>99% purity, 20 μg) was incubated at room temperature for 1 h with 30 nM [^{3}H]dihydrorotenone, a frequently used radiolabeled derivative of rotenone (2). The mixture was absorbed by prewetted DEAE-cellulose filter discs, which were subsequently washed extensively to remove unbound radioactivity. The same amount of bovine serum albumin was used to measure nonspecific binding, which was subtracted from total binding to derive specific binding. As shown in Fig. 4*D*, [^{3}H]dihydrorotenone was strongly bound to purified tubulin *in vitro*. This binding was almost completely blocked by preincubation of tubulin with unlabeled rotenone or colchicine (a 200-fold molar excess of [^{3}H]dihydrorotenone) or heat inactivation of tubulin (100 °C for 5 min). These results suggest that rotenone binds directly to tubulin on the colchicine site, as previous studies have indicated (4, 5). To assess the affinity of the binding between rotenone and tubulin, we performed the same assay with increasing concentrations of [^{3}H]dihydrorotenone. As shown in Fig. 4*E*, [^{3}H]dihydrorotenone bound to tubulin in a dose-dependent and saturable manner. Scatchard analysis of the data from three separate experiments showed that the K_d of this interaction was 22.4 ± 2.8 nM (Fig. 4*F*).

Rotenone-induced Microtubule Depolymerization Leads to Accumulation of Vesicles in the Soma—Microtubule depolymerization disrupts vesicular transport, which in the case of dopaminergic neurons would result in accumulation of dopamine vesicles in the soma. Leakage of dopamine from these vesicles (16, 17) would lead to increased DA oxidation and oxidative stress (18). To test this model, we treated midbrain neuronal cultures with or without rotenone (20 nM for 12 h) and co-stained them with antibodies against synaptophysin and TH. In control cells shown in the merged image in Fig. 5*A*, synaptophysin puncta were observed in the soma as well as in the processes in both TH$^+$ and TH$^-$ neurons. The amount of synaptophysin puncta in the soma was minimal (*inset 1* of Fig. 5*A*). After rotenone treatment, significantly more synaptophysin puncta were seen in the cell body in both types of neurons (Fig. 5*B*). Co-application of taxol (10 μM) blocked the rotenone-induced increase of synaptophysin puncta (Fig. 5*C*). Application of colchicine (10 μM for 12 h) also increased synaptophysin puncta in the cell body (Fig. 5*E*). This effect was greatly attenuated by taxol co-treatment (Fig. 5*F*), whereas taxol alone (Fig. 5*D*) did not cause any obvious change compared with the control.

We quantified the effects on synaptophysin localization by the ratio of its fluorescence signal in the soma to the area of the cell body. Because there was no significant difference between TH$^+$ and TH$^-$ neurons regarding this parameter, we measured the effect in all cells. As shown in Fig. 5*G*, rotenone induced a marked increase in this ratio in comparison to the control ($p < 0.001$, $n = 3$ coverslips for each condition). The effect was significantly attenuated by taxol ($p < 0.001$, $n = 3$). Colchicine had an effect similar to that of rotenone, which was also blocked by taxol ($p < 0.001$ *versus* colchicine alone, $n = 3$). Because almost all secretory vesicles are transported along microtubules (6) and would, thus, be affected by microtubule depolymerization, we examined the subcellular localization of syntaxin I, a t-SNARE (soluble NSF *N*-ethylmaleimide factor attachment) protein destined for the plasma membrane including that on the presynaptic terminal (19). As summarized in Fig. 5*H*, rotenone or colchicine induced a significant increase of syntaxin I puncta in the soma ($p < 0.001$ *versus* control, $n = 3$). The effects were significantly blocked by the co-application of taxol ($p < 0.001$ *versus* the corresponding treatment without taxol, $n = 3$).

The accumulation of vesicles in response to rotenone or colchicine correlated with apoptosis of TH$^+$ neurons in the midbrain culture. When we co-stained treated cultures for TUNEL (*red*), TH (*green*), and synaptophysin (*blue*), it was clear that TH$^+$ neurons undergoing apoptosis also exhibited strong accumulation of synaptophysin puncta (Fig. 5, *B* and *E*, *insets 2*). Neurons that were negative for TUNEL did not show significant vesicle accumulation (Fig. 5, *A*, *C*, *D*, and *F*, *insets 2*).

Rotenone-induced Microtubule Depolymerization Increases Oxidative Stress from Dopamine Metabolism—In DA neurons, leakage of dopamine from vesicles (16, 17) accumulated in the soma would lead to increased dopamine oxidation and oxidative stress (18). To test this hypothesis we measured the amount of protein carbonyls in midbrain neuronal cultures treated with rotenone, colchicine, taxol, or their combinations (each at 10 μM for 4 h). As shown in Fig. 6*A*, rotenone induced a strong increase in protein carbonyls ($p < 0.001$ *versus* control, $n = 5$ experiments), which was significantly attenuated by taxol co-treatment ($p < 0.05$ *versus* rotenone alone, $n = 5$). Colchicine caused a similar increase in protein carbonyls ($p < 0.001$ *versus* control, $n = 5$) that was completely blocked by taxol ($p > 0.14$, colchicine plus taxol *versus* con-

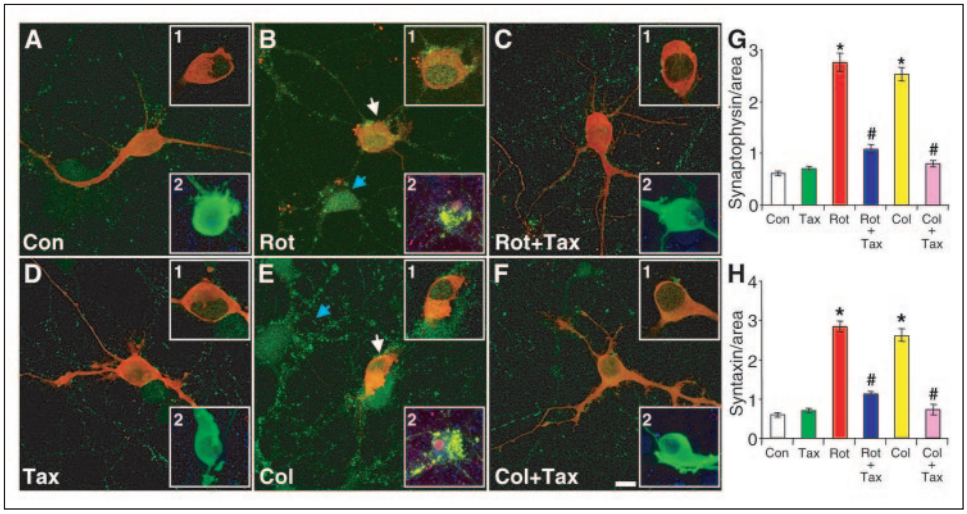

FIGURE 5. **Rotenone-induced microtubule depolymerization led to vesicle accumulation in the soma.** *A–F*, midbrain neuronal cultures were treated for 12 h without (*A*) or with (*B*) 20 nM rotenone (*Rot*), 20 nM rotenone plus 10 μM taxol (*Tax*; *C*), 10 μM taxol alone (*D*), 10 μM colchicine (*Col*; *E*) or 10 μM colchicine and taxol (*F*). *Con*, control. They were co-stained with anti-TH (*red*) and anti-synaptophysin (*green*). A stack of confocal images along the *z* axis was merged to show the accumulation of synaptophysin puncta in the soma. One section in the middle of the cell body was displayed in *insets 1* to show synaptophysin puncta inside the soma. Neurons were also co-stained for TUNEL (*red*), TH (*green*), and synaptophysin (*blue*) to show the correlation of vesicle accumulation and apoptosis in *insets 2*. *White* or *blue arrows*, synaptophysin puncta in TH^+ or TH^- neurons, respectively; *bar*, 10 μm. *G* and *H*, the intensity of synaptophysin (*G*) or syntaxin (*H*) signals divided by the area of the cell body was plotted for each treatment in (*A–F*). *, $p < 0.001$ *versus* control; #, $p < 0.001$ *versus* the corresponding single treatment without taxol. At least 3 coverslips were examined for each condition, with more than 10 TH^+ neurons and 10 TH^- neurons analyzed for each coverslip.

trol, $n = 5$). Taxol induced a partial but significant reduction in the amount of protein carbonyls elevated by rotenone. This is consistent with our results that rotenone acted on microtubules as well as complex I. Taxol itself had no effect on the amount of protein carbonyls. Similar results were obtained when we treated freshly cut adult rat midbrain slices with the same panel of drugs (all at 10 μM) for 2 h (Fig. 6*B*). Thus, results from midbrain neuronal cultures and midbrain slices suggest that rotenone-induced microtubule depolymerization leads to greater oxidative stress.

Next, we examined whether oxidative stress increased by rotenone was dependent on dopamine metabolism. As shown in Fig. 6*C*, co-application of α-methyl-*p*-tyrosine (α-MT), a specific inhibitor of tyrosine hydroxylase, the rate-limiting enzyme in the synthesis of dopamine, significantly decreased the amount of protein carbonyls elevated by rotenone ($p < 0.01$ *versus* rotenone alone, $n = 5$). NSD-1015, which specifically inhibits L-aromatic amino acid decarboxylase, the enzyme catalyzing the second step in the dopamine synthetic pathway, also significantly attenuated the rotenone-induced increase in protein carbonylation ($p < 0.01$ *versus* rotenone alone, $n = 5$). On the other hand, blocking the catabolism of dopamine with the monoamine oxidase A inhibitor clorgyline significantly reduced the level of protein carbonyls increased by rotenone ($p < 0.01$ *versus* rotenone alone, $n = 5$). Co-application of the antioxidant *N*-acetyl-L-cysteine significantly lowered the amount of protein carbonyls from the level induced by rotenone ($p < 0.05$ *versus* rotenone alone, $n = 5$). Similar results were obtained when we treated rat midbrain slices with rotenone in the absence or presence of these dopamine metabolism inhibitors (Fig. 6*D*). Furthermore, colchicine-induced increase in protein carbonyls was also significantly attenuated by blocking dopamine synthesis, degradation, or of reactive oxygen species (ROS) production in midbrain neuronal cultures (Fig. 6*E*, $p < 0.05$ *versus* colchicine alone, $n = 5$) or midbrain slices (Fig. 6*F*, $p < 0.05$ *versus* colchicine alone, $n = 5$). Together, the above results suggest that microtubule depolymerization induced by rotenone or colchicine leads to increased oxidative stress, most likely from enhanced oxidation of dopamine leaked from vesicles that are accumulated in the soma.

Rotenone Toxicity Is Dependent on Oxidation of Cytosolic Dopamine—The above results suggested that blocking dopamine synthesis or degradation might inhibit rotenone toxicity. Furthermore, treating neuronal cultures with antioxidants should also reduce cell death if the ROS produced during DA oxidation is a key factor. To test these possibilities, we treated midbrain neuronal cultures with rotenone alone or in combination with dopamine metabolism inhibitors or antioxidants. As shown in Fig. 7A, co-application of the TH inhibitor α-methyl-*p*-tyrosine significantly attenuated apoptosis induced by rotenone. A similar effect was observed for NSD-1015, an inhibitor of L-aromatic amino acid decarboxylase, the second enzyme on the dopamine synthetic pathway. Inhibition of monoamine oxidases (MAOs), which catalyze the oxidative degradation of dopamine, also significantly reduced rotenone toxicity. Furthermore, application of the antioxidants *N*-acetyl-L-cysteine or 2-methyl-*N*-(phenylmethylene)-2-propanamine *N*-oxide significantly decreased rotenone toxicity. With the exception of MAO-B inhibitor pargyline, the same panel of agents also significantly attenuated the selective toxicity of colchicine on TH^+ neurons (Fig. 7*B*). The lack of effect for the MAO-B inhibitor is consistent with the predominant expression of monoamine oxidase A, rather than MAO-B, in dopaminergic neurons (20).

These results suggest that oxidation of dopamine leaked from vesicles accumulated in the soma is critical for the specific toxicity of microtubule-depolymerizing agents such as rotenone and colchicine. To further test this idea, we used reserpine to block vesicular monoamine transporter 2 (VMAT2), which is responsible for the uptake of cytosolic dopamine into the vesicles (18). This would significantly increase cytosolic dopamine concentration while depleting vesicular DA pool (18). As shown in Fig. 7*C*, application of reserpine caused significant apoptosis of TH^+ neurons. The toxicity was significantly attenuated by inhibitors of dopamine synthesis or degradation and by antioxidants as well ($p < 0.01$, *versus* reserpine alone, $n = 5\sim8$). In contrast, microtubule drugs (colchicine or taxol) had no significant effect on reserpine toxicity ($p > 0.25$, *versus* reserpine alone, $n = 5\sim8$). Because reserpine had depleted dopamine in the vesicles, microtubule depolymerization or stabilization would no longer contribute to cell death. Reserpine had no

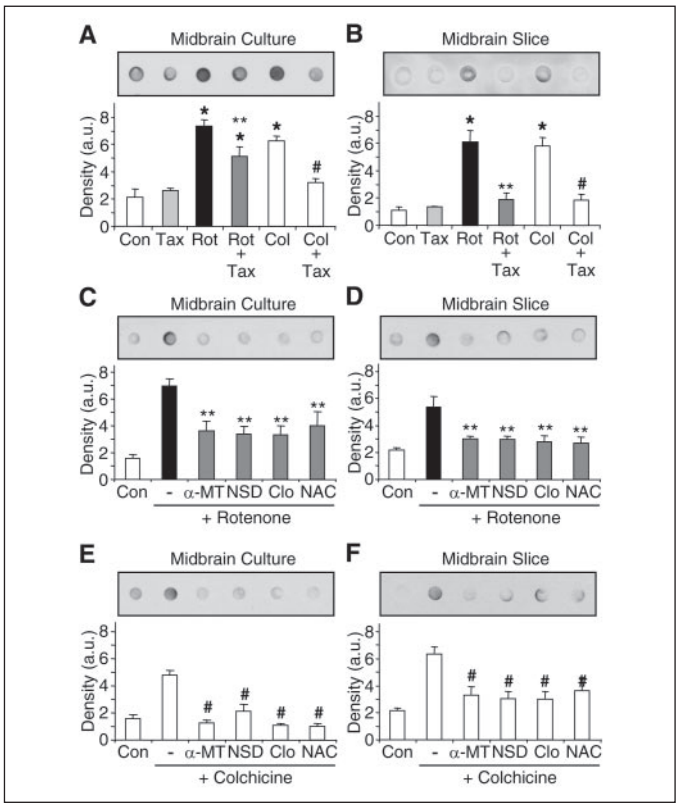

FIGURE 6. **Rotenone-induced microtubule depolymerization increased oxidative stress from dopamine metabolism.** *A*, *C*, and *E*, midbrain neuronal cultures were treated with various agents indicated (all at 10 μM for 4 h). *B*, *D*, and *F*, freshly cut rat midbrain slices were treated with the same panel of agents (all at 10 μM) for 2 h. The amount of protein carbonyls was measured by Oxyblot and quantified from five independent experiments. *a.u.*, arbitrary units. *A* and *B*, microtubule stabilization by taxol (*Tax*) significantly decreased the amount of protein carbonyls elevated by rotenone (*Rot*) or colchicine (*Col*) in midbrain cultures (*A*) and midbrain slices (*B*). *, $p < 0.01$ *versus* control (*Con*); **, $p < 0.05$ *versus* rotenone alone; #, $p < 0.01$ *versus* colchicine alone (Col). *C* and *D*, inhibiting dopamine synthesis by α-methyl-*p*-tyrosine (*α-MT*; TH inhibitor) or NSD-1015 (NSD, L-aromatic amino acid decarboxylase inhibitor), blocking dopamine oxidation by clorgyline (*Clo*, monoamine oxidase A inhibitor), or application of antioxidant *N*-acetyl-L-cysteine (*NAC*) significantly attenuated oxidative stress increased by rotenone in midbrain cultures (*C*) and midbrain slices (*D*). **, $p < 0.05$ *versus* rotenone alone. *E* and *F*, inhibitors of dopamine metabolism or antioxidant also significantly reduced oxidative stress elevated by colchicine in midbrain cultures (*E*) and midbrain slices (*F*). #, $p < 0.05$ *versus* colchicine alone.

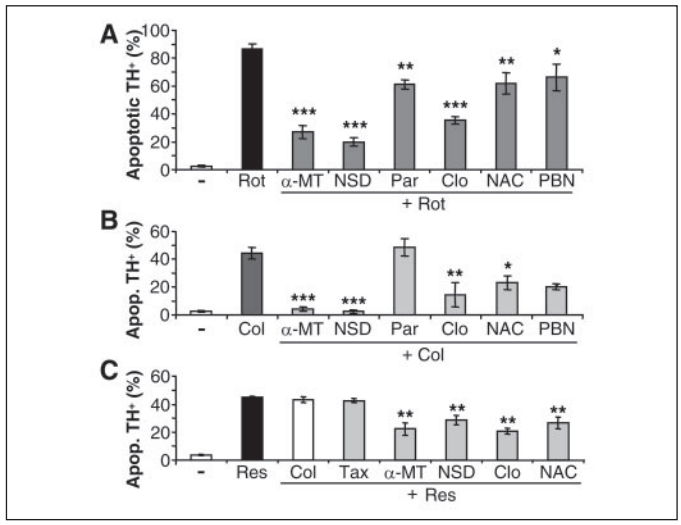

FIGURE 7. **Rotenone toxicity was dependent on dopamine metabolism.** *A*, midbrain neuronal cultures were treated for 12 h without (−) or with 10 μM rotenone (*Rot*) in the absence or presence of 1 mM α-methyl-*p*-tyrosine (*α-MT*; TH inhibitor), 1 μM NSD-1015 (L-aromatic amino acid decarboxylase inhibitor), 10 μM pargyline (*Par*; MAO-B inhibitor), 10 μM clorgyline (*Clo*; monoamine oxidase A inhibitor), 1 mM *N*-acetyl-L-cysteine (*NAC*; antioxidant), or 1 mM 2-methyl-*N*-(phenylmethylene)-2-propanamine *N*-oxide (*PBN*) (antioxidant). Fixed cultures were stained for TH, NeuN and TUNEL. The percentage of apoptotic TH^+ neurons was plotted for each treatment. *, $p < 0.05$; **, $p < 0.01$; ***, $p < 0.001$, all *versus* rotenone alone (Rot), $n = 3$ coverslips for each condition. *B*, the same experiments were performed with 10 μM colchicine (*Col*) replacing rotenone. Blocking dopamine synthesis, oxidation, or the production of ROS greatly reduced the death of TH^+ neurons induced by the microtubule-depolymerizing agent colchicine. The lack of significant effect for pargyline is due to the low level of MAO-B in catecholaminergic neurons. *, $p < 0.05$; **, $p < 0.01$; ***, $p < 0.001$, all *versus* colchicine alone, $n = 3\sim4$ coverslips for each condition. *C*, inhibition of vesicular dopamine uptake by reserpine (*Res*, 10 μM for 12 h) caused selective apoptosis of TH^+ neurons, which was not affected by co-treatment with colchicine or taxol but was significantly reduced by blocking dopamine synthesis, oxidation, or ROS production. **, $p < 0.01$ *versus* reserpine alone, $n = 5\sim8$ coverslips for each condition.

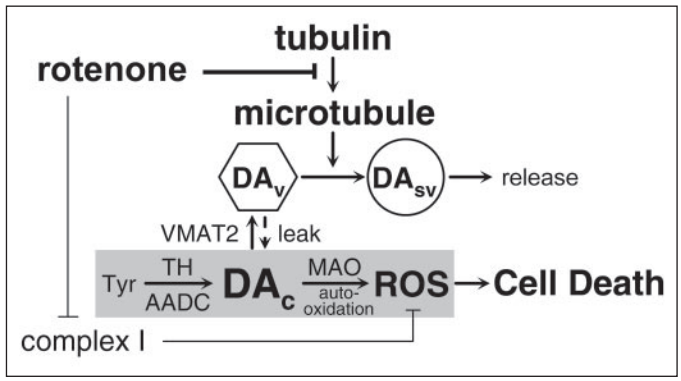

FIGURE 8. **A model illustrating the role of microtubule depolymerization in the selective toxicity of rotenone against dopaminergic neurons.** By depolymerizing microtubules, rotenone disrupts the transport of DA vesicles, which results in their accumulation in the soma and, therefore, an increase in cytosolic DA concentration due to the leakage of vesicles. ROS produced by increased oxidation of DA in combination with those generated by complex I inhibition make DA neurons much more vulnerable. DA metabolism (*shaded gray*) underlies the selectivity of rotenone toxicity. *Arrows*, positive effects; *blunted bars*, negative effects; DA_v, DA_{sv}, and DA_c, vesicular, synaptic vesicle, or cytosolic dopamine, respectively. *AADC*, L-aromatic amino acid decarboxylase.

significant toxicity on TH^- neurons (6.5 ± 1.7%, $n = 11$), as VMAT2 is only expressed in monoaminergic neurons (18). Very similar results were obtained with tetrabenazine, another specific inhibitor of VMAT2 (data not shown).

DISCUSSION

The present data support a model (Fig. 8) that could explain the selective vulnerability of dopaminergic neurons to rotenone. By inhibiting complex I in the mitochondrial respiratory chain, rotenone produces ROS in all types of cells (21). Although the microtubule-depolymerizing activity of rotenone is not cell type-specific either, it significantly contributes to the selective death of DA neurons because it disrupts microtubule-based transport of dopamine vesicles. This results in vesicle accumulation in the soma, which leads to increased oxidative stress due to oxidation of dopamine leaked from the vesicles (16, 17). Thus, the combination of both activities of rotenone would generate far more ROS in DA neurons than in other types of cells, rendering these neurons particularly vulnerable to this environmental PD toxin.

In addition to dopaminergic neurons, TH^+ neurons in midbrain cultures also contained small numbers of epinephrinergic or norepinephrinergic neurons, which were already included in our studies. Thus, catecholaminergic neurons that depend on long range microtubule-based transport to move their oxidizable cargoes are vulnerable to microtubule-depolymerizing agents such as rotenone or colchicine. Neurons that do not synthesize an oxidizable neurotransmitter, such as glutamatergic or GABAergic neurons, were much less susceptible to rotenone toxicity (Fig. 1*G*), even though vesicles were also accumulated in their soma after disruption of microtubules (see Fig. 5, *B* and *E*). In

fact, the K_m values of VMAT2 for catecholamines are around 0.2 μM, whereas the K_m values for vesicular uptake of glutamate or GABA range from 0.3 to ~3 mM (18). This >1000-fold difference in the affinity of vesicular transporters toward various neurotransmitters ensures that the cytosolic concentration of catecholamines is much lower than that of other neurotransmitters, which greatly minimizes the oxidation of cytosolic catecholamines either by MAOs or auto-oxidation.

Previous studies using the yeast single subunit complex I gene NDI1 have shown that complex I inhibition appears to fully account for the toxicity of rotenone on cell lines such as PC12 and SK-N-MC (22, 23). The discrepancy with our results, which illustrate the important contributions of microtubule-depolymerizing activity of rotenone, may be due to the differences between these cell lines and TH^+ neurons in our midbrain neuronal cultures. These cell lines only have very short neurite-like protrusions, which are very different from the elaborate, long processes of DA neurons. We routinely observed axons with length of 1–2 mm in TH^+ neurons in our cultures, which were quite comparable with the length of TH^+ nigrostriatal projections (4–6 mm) in sagittal sections from adult rat brains. Consequently, the microtubule-depolymerizing activity of rotenone would have a much higher impact on TH^+ neurons than on the cell lines. Furthermore, the cell lines are much less "dopaminergic" in that they do not have similar mechanisms for the synthesis, storage, transport, reuptake, and degradation of dopamine like those in TH^+ neurons in midbrain neuronal cultures.

Although the model illustrated in Fig. 8 could explain why short projection DA neurons, such as those in retina, are not significantly affected in PD, it cannot explain why nigral DA neurons are much more vulnerable than those in the ventral tagmental area both in human PD patients and in the rotenone model of the disease (2). Nigral and the ventral tagmental area dopaminergic neurons both have very long axons enriched in microtubules. Other factors, such as the ratio of DAT and VMAT2 expression levels (24), the existence of neuromelanin (25), and the enrichment of iron (26) in nigral DA neurons, may render them more susceptible to harmful agents, either environmental or endogenous, than DA neurons in the ventral tagmental area.

It may not be a coincidence that MPP^+, the active metabolite of the experimental PD toxin MPTP, also inhibits complex I (27) and depolymerizes microtubules (28, 29) just like rotenone does (3–5). Further studies are necessary to examine the involvement of microtubule depolymerization in the selective toxicity of other PD toxins, such as the pesticide paraquat, which is strongly implicated in PD and is structurally similar to MPP^+ (30, 31). Our results provide the first evidence that microtubule depolymerization plays a critical role in the specific death of dopaminergic neurons induced by an environmental toxin linked to Parkinson disease.

REFERENCES

1. Langston, J. W. (2002) *Neurotoxicology* **23,** 443–450
2. Betarbet, R., Sherer, T. B., MacKenzie, G., Garcia-Osuna, M., Panov, A. V., and Greenamyre, J. T. (2000) *Nat. Neurosci.* **3,** 1301–1306
3. Chance, B., Williams, G. R., and Hollunger, G. (1963) *J. Biol. Chem.* **238,** 418–431
4. Brinkley, B. R., Barham, S. S., Barranco, S. C., and Fuller, G. M. (1974) *Exp. Cell Res.* **85,** 41–46
5. Marshall, L. E., and Himes, R. H. (1978) *Biochim. Biophys. Acta* **543,** 590–594
6. Goldstein, L. S. (2003) *Neuron* **40,** 415–425
7. Hastings, T. G., Lewis, D. A., and Zigmond, M. J. (1996) *Proc. Natl. Acad. Sci. U. S. A.* **93,** 1956–1961
8. Ren, Y., Zhao, J. H., and Feng, J. (2003) *J. Neurosci.* **23,** 3316–3324
9. Zhao, J., Ren, Y., Jiang, Q., and Feng, J. (2003) *J. Cell Sci.* **116,** 4011–4019
10. Feng, J., Yan, Z., Ferreira, A., Tomizawa, K., Liauw, J. A., Zhuo, M., Allen, P. B., Ouimet, C. C., and Greengard, P. (2000) *Proc. Natl. Acad. Sci. U. S. A.* **97,** 9287–9292
11. Jiang, H., Ren, Y., Zhao, J., and Feng, J. (2004) *Hum. Mol. Genet.* **13,** 1745–1754
12. Joshi, H. C., and Cleveland, D. W. (1989) *J. Cell Biol.* **109,** 663–673
13. Himes, R. H., Burton, P. R., Kersey, R. N., and Pierson, G. B. (1976) *Proc. Natl. Acad. Sci. U. S. A.* **73,** 4397–4399
14. Borisy, G. G. (1972) *Anal. Biochem.* **50,** 373–385
15. Tse, C., and Doherty, R. A. (1980) *J. Neurochem.* **35,** 767–774
16. Floor, E., Leventhal, P. S., Wang, Y., Meng, L., and Chen, W. (1995) *J. Neurochem.* **64,** 689–699
17. Eisenhofer, G., Kopin, I. J., and Goldstein, D. S. (2004) *Ann. N. Y. Acad. Sci.* **1018,** 224–230
18. Liu, Y., and Edwards, R. H. (1997) *Annu. Rev. Neurosci.* **20,** 125–156
19. Chen, Y. A., and Scheller, R. H. (2001) *Nat. Rev. Mol. Cell Biol.* **2,** 98–106
20. Shih, J. C., Chen, K., and Ridd, M. J. (1999) *Annu. Rev. Neurosci.* **22,** 197–217
21. Barrientos, A., and Moraes, C. T. (1999) *J. Biol. Chem.* **274,** 16188–16197
22. Seo, B. B., Nakamaru-Ogiso, E., Flotte, T. R., Yagi, T., and Matsuno-Yagi, A. (2002) *Mol. Ther.* **6,** 336–341
23. Sherer, T. B., Betarbet, R., Testa, C. M., Seo, B. B., Richardson, J. R., Kim, J. H., Miller, G. W., Yagi, T., Matsuno-Yagi, A., and Greenamyre, J. T. (2003) *J. Neurosci.* **23,** 10756–10764
24. Miller, G. W., Gainetdinov, R. R., Levey, A. I., and Caron, M. G. (1999) *Trends Pharmacol. Sci.* **20,** 424–429
25. Zecca, L., Zucca, F. A., Wilms, H., and Sulzer, D. (2003) *Trends Neurosci.* **26,** 578–580
26. Sofic, E., Paulus, W., Jellinger, K., Riederer, P., and Youdim, M. B. (1991) *J. Neurochem.* **56,** 978–982
27. Dauer, W., and Przedborski, S. (2003) *Neuron* **39,** 889–909
28. Cappelletti, G., Maggioni, M. G., and Maci, R. (1999) *J. Neurosci. Res.* **56,** 28–35
29. Cappelletti, G., Pedrotti, B., Maggioni, M. G., and Maci, R. (2001) *Cell Biol. Int.* **25,** 981–984
30. Thiruchelvam, M., Richfield, E. K., Baggs, R. B., Tank, A. W., and Cory-Slechta, D. A. (2000) *J. Neurosci.* **20,** 9207–9214
31. Di Monte, D. A. (2003) *Lancet Neurol.* **2,** 531–538